RF-induced heating of metallic implants simulated as PEC: Is there something missing?

Received: 14 May 2020 | Revised: 17 August 2020 | Accepted: 18 August 2020

DOI: 10.1002/mrm.28512

LETTER TO THE EDITOR

Magnetic Resonance in Medicine

RF-induced heating of metallic implants simulated as PEC: Is there something missing?

The possible heating of metallic devices implanted in the patient's body is a source of concern in MRI, discussed in many papers and standards.[1-15] Two fields may produce heating in the presence of metallic implants: gradient fields (which may deposit significant Joule losses within bulky metallic objects[16-20]) and radiofrequency (RF) fields. In the latter case, thermal effects are commonly evaluated in terms of specific absorption rate (SAR) around the implant and, sometimes, of the consequent heating.[21-28]

In most papers investigating the problem via simulations, metallic implants at RF are modeled as perfect electric conductors (PEC), forcing the electric and magnetic fields to be purely perpendicular and tangential, respectively, to the external surface of the implant, whose volume is removed from the computational domain.

As a drawback, the PEC approximation prevents from looking inside the object; thus, the simulation of the heating process misses the contribution coming from the power deposited by the field in the metallic volume. Moreover, when metallic implants are not described as PEC, but discretized into elements whose size is larger than the penetration depth (as done, for instance, in Refs. 24,27-28), the computation of the Joule losses deposited inside them cannot be considered as accurate, because the adopted mesh is unsuited to reconstruct the internal field pattern.

Many appliances exploit medium frequency magnetic fields to heat/anneal/melt metallic objects by direct dissipation of energy inside them.[29-30] In addition, for a given amplitude of the incident field, analytical solutions show a monotonic increase of the power deposited inside conductors as the frequency increases.[18] Hence, a curiosity about the amount of heating directly produced inside metallic implants by the MRI RF fields seems to be justified. To settle the question, we propose to combine the Surface Impedance Boundary Conditions (SIBC) and the Poynting vector. For good conductors at RF, the SIBC allow avoiding the extremely tiny discretization required to obtain a proper description of the field distribution within metallic objects, where the penetration depth (on the order of some tens of micrometers, at typical Larmor frequencies of MRI) would lead to very heavy computational burdens. At the same time, the SIBC provide the correct distribution of the electromagnetic field over the surface of the object.[31-36] Therefore, this distribution can be used to compute the complex Poynting vector, whose real part allows quantifying the amount of power locally deposited in a thin layer corresponding to the field penetration. The procedure, realized by us through the software COMSOL Multiphysics, has been validated by comparison with the analytical calculation of the power deposited inside a metallic sphere exposed to a homogeneous RF magnetic field,[18] obtaining an excellent agreement (discrepancy $< 0.2\%$). Figure 1A shows such a power and compares it to Finite Element (FE) solutions, for different resolutions. As reported, FE solutions converge to the reference value, but are not accurate until the resolution approaches the penetration depth. Moreover, the convergence may be non-monotonic.

Once validated, the proposed procedure has been applied to a realistic CoCrMo hip prosthesis (conductivity: 1.26 MS/m) embedded in a cylindrical phantom (with the properties defined in Ref. 12) exposed to the field of a birdcage working in circular polarization at 128 MHz (Figure 1B). The results have been scaled to get a partial-body SAR equal to the limit recommended in Ref. 11 for normal operating mode. Finally, thermal simulations have been performed using as driving terms, separately, the SAR around the implant and the power deposited inside it (see Figure 1C). After 6 minutes of exposure, the maximum heating (occurring at the tip of the stem, where, without the implant, SAR would have produced a heating around 0.25 K) was about 1 K. Less than 1% of this temperature elevation was due to the power deposited inside the prosthesis. The relative contribution to the heating due to the internal power reached a maximum of about 15% near the center of the stem, where the absolute temperature was much lower (<0.1 K), anyway. The test was repeated for a long femoral nail (length: 240 mm, diameter: 9 mm) in longitudinal position. After 6 minutes, the maximum heating (at the tip of the nail) was about 0.9 K and the contribution due to the internal power was lower than 1%. This confirms that the

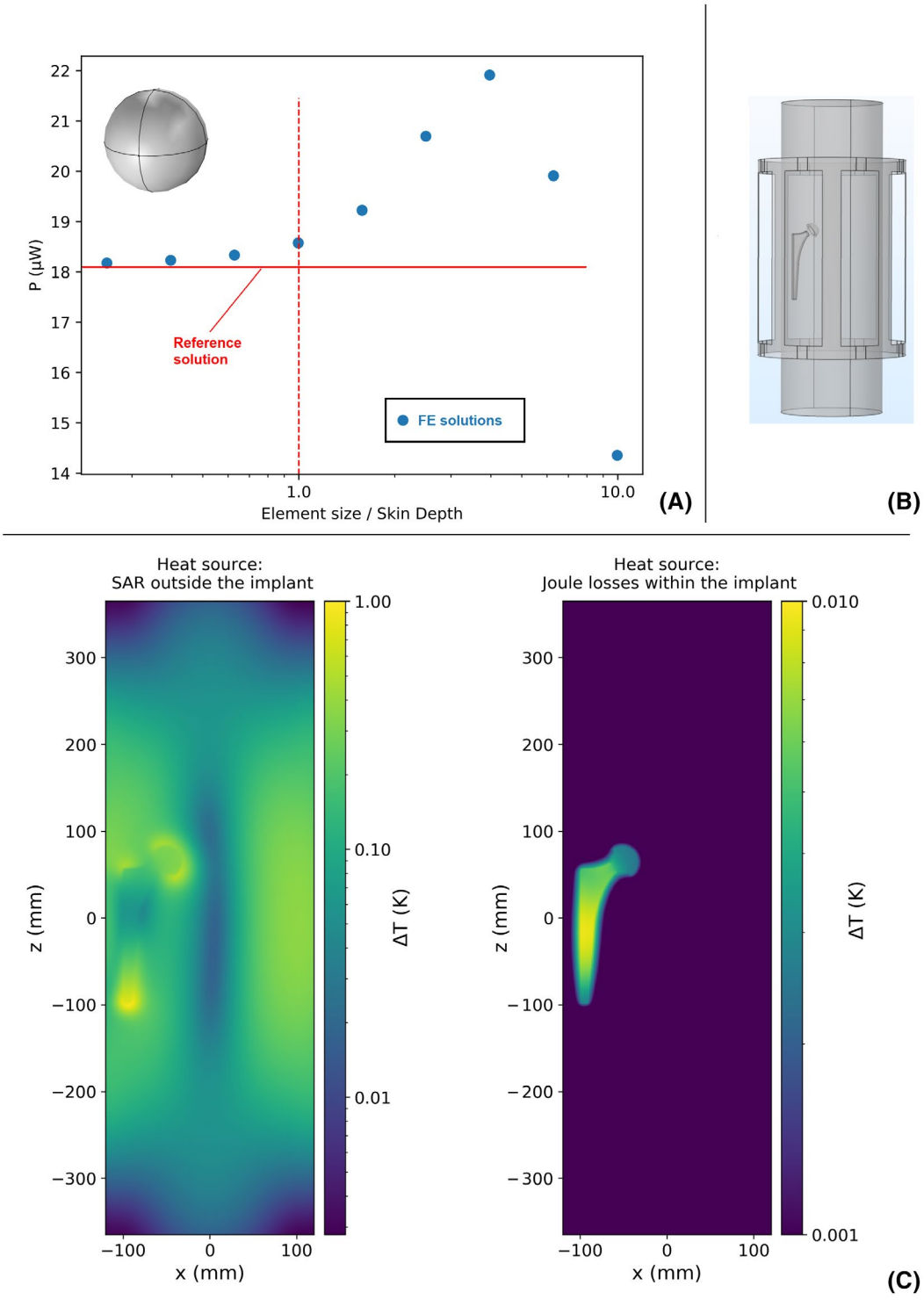

FIGURE 1 RF-induced heating of CoCrMo objects at 128 MHz, where the penetration depth is ~40 μm: A, Joule losses induced in a sphere (radius: 1 cm; applied magnetic flux density: 1.2 μT), computed with the proposed approach based on the SIBC and Poynting vector (red horizontal line) and with a Finite Element solver for different values of the element size (blue dots); B, scheme of the analyzed hip implant embedded in a gel phantom, radiated by a birdcage antenna; C, maps comparing the temperature increases of the hip implant continuously radiated for 6 min, using as heat source the SAR around the implant itself or the Joule losses deposited within it.

heating due to Joule losses within the implant at RF is negligible. Hence, on a practical side, PEC models are acceptable, as are previous results based on discretizations larger than the penetration depth.

ACKNOWLEDGMENTS

The results here presented have been developed in the framework of the 17IND01 MIMAS Project. This project has received funding from the EMPIR Programme, co-financed

by the Participating States and from the European Union's Horizon 2020 Research and Innovation Programme.

Luca Zilberti
Umberto Zanovello
Alessandro Arduino
Oriano Bottauscio
Mario Chiampi

Istituto Nazionale di Ricerca Metrologica, Torino, Italy

Correspondence
Luca Zilberti, Istituto Nazionale di Ricerca Metrologica, Strada delle Cacce 91, I- 10135, Torino, Italy.
Email: l.zilberti@inrim.it

ORCID

Luca Zilberti https://orcid.org/0000-0002-2382-4710

REFERENCES

1. Davis P, Crooks L, Arakawa M, McRee R, Kaufman L, Margulis A. Potential hazards in NMR imaging: Heating effects of changing magnetic fields and RF fields on small metallic implants. *Am J Roentgenol*. 1981;137:857-860.
2. Nutt J, Anderson V, Peacock JH, Hammerstad J, Burchiel K. DBS and diathermy interaction induces severe CNS damage. *Neurology*. 2001;56:1384-1386.
3. Dempsey MF, Condon B, Hadley DM. Investigation of the factors responsible for burns during MRI. *J Magn Reson Imaging*. 2001;13:627-631.
4. Spiegel J, Fuss G, Backens M, et al. Transient dystonia following magnetic resonance imaging in a patient with deep brain stimulation electrodes for the treatment of Parkinson disease: Case report. *J Neurosurg*. 2003;99:772-774.
5. Irnich W, Irnich B, Bartsch C, Stertmann WA, Gufler H, Weiler G. Do we need pacemakers resistant to magnetic resonance imaging? *EP Eur*. 2005;7:353-365.
6. Henderson JM, Tkach J, Phillips M, Baker K, Shellock FG, Rezai AR. Permanent neurological deficit related to magnetic resonance imaging in a patient with implanted deep brain stimulation electrodes for Parkinson's disease: Case report. *Neurosurg*. 2005;57:E1063.
7. Graf H, Steidle G, Schick F. Heating of metallic implants and instruments induced by gradient switching in a 1.5-Tesla whole-body unit. *J Magn Reson Imaging*. 2007;26:1328-1333.
8. Kanal E, Barkovich AJ, Bell C, et al. ACR guidance document on MR safe practices: 2013. *J Magn Reson Imaging*. 2013;37:501-530.
9. Bannan KE, Handler W, Chronik B, Salisbury SP. Heating of metallic rods induced by time-varying gradient fields in MRI. *J Magn Reson Imaging*. 2013;38:411-416.
10. Winter L, Seifert F, Zilberti L, Murbach M, Ittermann B. MRI-related heating of implants and devices: A review. *J Magn Reson Imaging*. 2020. https://doi.org/10.1002/jmri.27194
11. International Electrotechnical Commission (IEC). *Medical electrical equipment: Part 2–33. Particular requirements for the safety of magnetic resonance equipment for medical diagnosis. IEC 60601-2-33 ed. 3.2. Consolidated with amendments 1 and 2*. Geneva: IEC, 2015.
12. American Society of Testing and Materials (ASTM) International. *Standard Test Method for Measurement of Radio Frequency Induced Heating On or Near Passive Implants During Magnetic Resonance Imaging*. West Conshohocken, PA: ASTM International; ASTM F2182-11a. 2019.
13. International Organization for Standardization (ISO). *Assessment of the Safety of Magnetic Resonance Imaging for Patients with an Active Implantable Medical Device*. Geneva, Switzerland: Technical Specification ISO/TS 10974 second edition. 2018.
14. Food and Drug Administration (FDA). *Establishing Safety and Compatibility of Passive Implants in the Magnetic Resonance (MR) Environment—Guidance for Industry and Food and Drug Administration Staff*. Rockville, MD: Food and Drug Administration; 2014.
15. Food and Drug Administration (FDA). *Assessment of Radiofrequency-Induced Heating in the Magnetic Resonance (MR) Environment for Multi-Configuration Passive Medical Devices – Guidance for Industry and Food and Drug Administration Staff*. Rockville, MD: Food and Drug Administration; 2016.
16. Zilberti L, Bottauscio O, Chiampi M, Hand J, Lopez HS, Crozier S. Collateral thermal effect of MRI-LINAC gradient coils on metallic hip prostheses. *IEEE Trans Magn*. 2014;50:1-4.
17. Zilberti L, Bottauscio O, Chiampi M, et al. Numerical prediction of temperature elevation induced around metallic hip prostheses by traditional, split, and uniplanar gradient coils. *Magn Reson Med*. 2015;74:272-279.
18. Zilberti L, Arduino A, Bottauscio O, Chiampi M. The underestimated role of gradient coils in MRI safety. *Magn Reson Med*. 2017;77:13-15.
19. Brühl R, Ihlenfeld A, Ittermann B. Gradient heating of bulk metallic implants can be a safety concern in MRI. *Magn Reson Med*. 2017;77:1739-1740.
20. Arduino A, Bottauscio O, Brühl R, Chiampi M, Zilberti L. In silico evaluation of the thermal stress induced by MRI switched gradient fields in patients with metallic hip implant. *Phys Med Biol*. 2019;64:245006.
21. Nyenhuis JA, Park SM, Kamondetdacha R, Amjad A, Shellock FG, Rezai AR. MRI and implanted medical devices: Basic interactions with an emphasis on heating. *IEEE Trans Device Mater Reliab*. 2005;5:467-480.
22. Stenschke J, Li D, Thomann M, Schaefers G, Zylka W. A numerical investigation of RF heating effect on implants during MRI compared to experimental measurements. *Adv Med Eng*. 2007;114:53-58.
23. Mohsin SA, Sheikh NM, Abbas W. MRI induced heating of artificial bone implants. *J Electromagnet Wave*. 2009;23:799-808.
24. Powell J, Papadaki A, Hand J, Hart A, McRobbie D. Numerical simulation of SAR induced around Co-Cr-Mo hip prostheses in situ exposed to RF fields associated with 1.5 and 3 T MRI body coils. *Magn Reson Med*. 2012;68:960-968.
25. Liu Y, Chen J, Shellock FG, Kainz W. Computational and experimental studies of an orthopedic implant: MRI-related heating at 1.5-T/64-MHz and 3-T/128-MHz. *J Magn Reson Imaging*. 2013;37:491-497.
26. Murbach M, Zastrow E, Neufeld E, Cabot E, Kainz W, Kuster N. Heating and safety concerns of the radio-frequency field in MRI. *Curr Radiol Rep*. 2015;3:1-9.

27. Winter L, Oberacker E, Özerdem C, et al. On the RF heating of coronary stents at 7.0 Tesla MRI. *Magn Reson Med*. 2015;74:999-1010.
28. Destruel A, O'Brien K, Jin J, Liu F, Barth M, Crozier S. Adaptive SAR mass-averaging framework to improve predictions of local RF heating near a hip implant for parallel transmit at 7 T. *Magn Reson Med*. 2019;81:615-627.
29. Lucìa O, Maussion P, Dede E, Burdìo JM. Induction heating technology and its applications: Past developments, current technology, and future challenges. *IEEE Trans Ind Electron*. 2013;61:2509-2520.
30. Rudnev V, Loveless D, Cook RL. *Handbook of Induction Heating*. Boca Raton: CRC Press; 2017.
31. Fazwi TH, Taher Ahmed M, Burke PE. On the use of the impedance boundary conditions in eddy current problems. *IEEE Trans Magn*. 1985;21:1835-1840.
32. Jingguo W, Lavers JD, Peibai Z. Modified surface impedance boundary condition applied to eddy current problems. *IEEE Trans Magn*. 1992;28:1197-1200.
33. Jingguo W, Lavers JD. Modified surface impedance boundary conditions for 3D Eddy current problems. *IEEE Trans Magn*. 1993;29:1826-1829.
34. Jayasekera KASN, Ciric IR. Evaluation of surface impedance models for axisymmetric Eddy-current fields. *IEEE Trans Magn*. 2007;43:1991-2000.
35. Yuferev SV, Di Rienzo L. Surface impedance boundary conditions in terms of various formalisms. *IEEE Trans Magn*. 2010;46:3617-3628.
36. Yuferev SV, Ida N. *Surface Impedance Boundary Conditions A Comprehensive Approach*. Boca Raton: CRC Press; 2010.